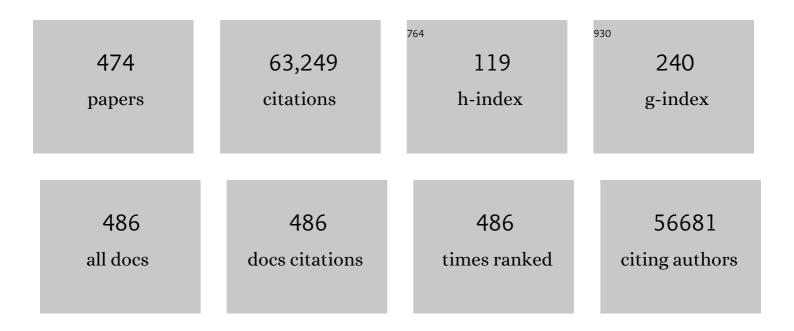
Pulickel M Ajayan

List of Publications by Year in descending order

Source: https://exaly.com/author-pdf/1592306/publications.pdf Version: 2024-02-01



Ριμιςκει Μ Διαναν

#	Article	IF	CITATIONS
1	High-efficiency two-dimensional Ruddlesden–Popper perovskite solar cells. Nature, 2016, 536, 312-316.	13.7	2,767
2	Large Scale Growth and Characterization of Atomic Hexagonal Boron Nitride Layers. Nano Letters, 2010, 10, 3209-3215.	4.5	2,317
3	Exfoliated Graphitic Carbon Nitride Nanosheets as Efficient Catalysts for Hydrogen Evolution Under Visible Light. Advanced Materials, 2013, 25, 2452-2456.	11.1	2,227
4	Atomic layers of hybridized boron nitride and graphene domains. Nature Materials, 2010, 9, 430-435.	13.3	2,002
5	Vertical and in-plane heterostructures from WS2/MoS2 monolayers. Nature Materials, 2014, 13, 1135-1142.	13.3	1,918
6	Intrinsic Structural Defects in Monolayer Molybdenum Disulfide. Nano Letters, 2013, 13, 2615-2622.	4.5	1,766
7	Vapour phase growth and grain boundary structure of molybdenum disulphide atomic layers. Nature Materials, 2013, 12, 754-759.	13.3	1,590
8	Largeâ€Area Vaporâ€Phase Growth and Characterization of MoS ₂ Atomic Layers on a SiO ₂ Substrate. Small, 2012, 8, 966-971.	5.2	1,556
9	Atomic cobalt on nitrogen-doped graphene for hydrogen generation. Nature Communications, 2015, 6, 8668.	5.8	1,356
10	Defects Engineered Monolayer MoS ₂ for Improved Hydrogen Evolution Reaction. Nano Letters, 2016, 16, 1097-1103.	4.5	1,015
11	Wetting transparency of graphene. Nature Materials, 2012, 11, 217-222.	13.3	971
12	In-plane heterostructures of graphene and hexagonal boron nitride with controlled domain sizes. Nature Nanotechnology, 2013, 8, 119-124.	15.6	796
13	A subthermionic tunnel field-effect transistor with an atomically thin channel. Nature, 2015, 526, 91-95.	13.7	793
14	Atomically dispersed platinum supported on curved carbon supports for efficient electrocatalytic hydrogen evolution. Nature Energy, 2019, 4, 512-518.	19.8	756
15	Chemical Vapor Deposition Growth of Crystalline Monolayer MoSe ₂ . ACS Nano, 2014, 8, 5125-5131.	7.3	694
16	High Efficiency Photocatalytic Water Splitting Using 2D αâ€Fe ₂ O ₃ /gâ€C ₃ N ₄ Zâ€6cheme Catalysts. Advanced Ene Materials, 2017, 7, 1700025.	ergy 10.2	664
17	Composites with carbon nanotubes and graphene: An outlook. Science, 2018, 362, 547-553.	6.0	662
18	Room-temperature ferroelectricity in CulnP2S6 ultrathin flakes. Nature Communications, 2016, 7, 12357.	5.8	637

#	Article	IF	CITATIONS
19	Fracture toughness of graphene. Nature Communications, 2014, 5, 3782.	5.8	567
20	Light-induced lattice expansion leads to high-efficiency perovskite solar cells. Science, 2018, 360, 67-70.	6.0	554
21	Achieving Highly Efficient, Selective, and Stable CO ₂ Reduction on Nitrogen-Doped Carbon Nanotubes. ACS Nano, 2015, 9, 5364-5371.	7.3	546
22	Second harmonic microscopy of monolayer MoS <mml:math xmlns:mml="http://www.w3.org/1998/Math/MathML" display="inline"><mml:msub><mml:mrow /><mml:mn>2</mml:mn></mml:mrow </mml:msub>. Physical Review B, 2013, 87, .</mml:math 	1.1	539
23	Ultrathin high-temperature oxidation-resistant coatings of hexagonal boron nitride. Nature Communications, 2013, 4, 2541.	5.8	536
24	Graphene-Based Standalone Solar Energy Converter for Water Desalination and Purification. ACS Nano, 2018, 12, 829-835.	7.3	519
25	A metal-free electrocatalyst for carbon dioxide reduction to multi-carbon hydrocarbons and oxygenates. Nature Communications, 2016, 7, 13869.	5.8	505
26	Charge-transfer-based Gas Sensing Using Atomic-layer MoS2. Scientific Reports, 2015, 5, 8052.	1.6	489
27	Two-Step Growth of Two-Dimensional WSe ₂ /MoSe ₂ Heterostructures. Nano Letters, 2015, 15, 6135-6141.	4.5	479
28	Controlled nanocutting of graphene. Nano Research, 2008, 1, 116-122.	5.8	472
29	Direct Growth of Graphene/Hexagonal Boron Nitride Stacked Layers. Nano Letters, 2011, 11, 2032-2037.	4.5	466
30	Band Gap Engineering and Layer-by-Layer Mapping of Selenium-Doped Molybdenum Disulfide. Nano Letters, 2014, 14, 442-449.	4.5	463
31	Three-dimensionally bonded spongy graphene material with super compressive elasticity and near-zero Poisson's ratio. Nature Communications, 2015, 6, 6141.	5.8	458
32	Strain and structure heterogeneity in MoS2 atomic layers grown by chemical vapour deposition. Nature Communications, 2014, 5, 5246.	5.8	453
33	Liquid Phase Exfoliation of Two-Dimensional Materials by Directly Probing and Matching Surface Tension Components. Nano Letters, 2015, 15, 5449-5454.	4.5	436
34	Incorporation of Nitrogen Defects for Efficient Reduction of CO ₂ via Two-Electron Pathway on Three-Dimensional Graphene Foam. Nano Letters, 2016, 16, 466-470.	4.5	435
35	Deep eutectic solvents for cathode recycling of Li-ion batteries. Nature Energy, 2019, 4, 339-345.	19.8	422
36	Nitrogenâ€Doped Carbon Nanotube Arrays for Highâ€Efficiency Electrochemical Reduction of CO ₂ : On the Understanding of Defects, Defect Density, and Selectivity. Angewandte Chemie - International Edition, 2015, 54, 13701-13705.	7.2	382

#	Article	IF	CITATIONS
37	Two-dimensional van der Waals materials. Physics Today, 2016, 69, 38-44.	0.3	381
38	Oxygenated monolayer carbon nitride for excellent photocatalytic hydrogen evolution and external quantum efficiency. Nano Energy, 2016, 27, 138-146.	8.2	379
39	Highly Sensitive Detection of Polarized Light Using Anisotropic 2D ReS ₂ . Advanced Functional Materials, 2016, 26, 1169-1177.	7.8	376
40	Strategies for Dendriteâ€Free Anode in Aqueous Rechargeable Zinc Ion Batteries. Advanced Energy Materials, 2020, 10, 2001599.	10.2	376
41	Electrochemical CO ₂ Reduction with Atomic Ironâ€Dispersed on Nitrogenâ€Doped Graphene. Advanced Energy Materials, 2018, 8, 1703487.	10.2	369
42	Direct Ink Writing: A 3D Printing Technology for Diverse Materials. Advanced Materials, 2022, 34, e2108855.	11.1	361
43	Pyridinicâ€Nitrogenâ€Dominated Graphene Aerogels with Fe–N–C Coordination for Highly Efficient Oxygen Reduction Reaction. Advanced Functional Materials, 2016, 26, 5708-5717.	7.8	360
44	Full-color fluorescent carbon quantum dots. Science Advances, 2020, 6, .	4.7	344
45	Self-optimizing, highly surface-active layeredÂmetal dichalcogenide catalysts for hydrogen evolution. Nature Energy, 2017, 2, .	19.8	336
46	Emerging Applications of Elemental 2D Materials. Advanced Materials, 2020, 32, e1904302.	11.1	336
47	Optoelectronic crystal of artificial atoms in strain-textured molybdenum disulphide. Nature Communications, 2015, 6, 7381.	5.8	331
48	Multisegmented Au-MnO ₂ /Carbon Nanotube Hybrid Coaxial Arrays for High-Power Supercapacitor Applications. Journal of Physical Chemistry C, 2010, 114, 658-663.	1.5	314
49	Ultrafast formation of interlayer hot excitons in atomically thin MoS2/WS2 heterostructures. Nature Communications, 2016, 7, 12512.	5.8	313
50	Exfoliation of a non-van der Waals material from iron ore hematite. Nature Nanotechnology, 2018, 13, 602-609.	15.6	295
51	Wafer-scale monodomain films of spontaneously aligned single-walled carbon nanotubes. Nature Nanotechnology, 2016, 11, 633-638.	15.6	292
52	Two-dimensional non-volatile programmable p–n junctions. Nature Nanotechnology, 2017, 12, 901-906.	15.6	278
53	Design Considerations for Unconventional Electrochemical Energy Storage Architectures. Advanced Energy Materials, 2015, 5, 1402115.	10.2	271
54	High temperature electrical energy storage: advances, challenges, and frontiers. Chemical Society Reviews, 2016, 45, 5848-5887.	18.7	268

#	Article	IF	CITATIONS
55	Stable Lightâ€Emitting Diodes Using Phaseâ€Pure Ruddlesden–Popper Layered Perovskites. Advanced Materials, 2018, 30, 1704217.	11.1	258
56	An Atomically Layered InSe Avalanche Photodetector. Nano Letters, 2015, 15, 3048-3055.	4.5	253
57	Temperature dependence of radial breathing mode Raman frequency of single-walled carbon nanotubes. Physical Review B, 2002, 66, .	1.1	250
58	Unveiling Active Sites for the Hydrogen Evolution Reaction on Monolayer MoS ₂ . Advanced Materials, 2017, 29, 1701955.	11.1	249
59	A Bottomâ€Up Approach to Build 3D Architectures from Nanosheets for Superior Lithium Storage. Advanced Functional Materials, 2014, 24, 125-130.	7.8	247
60	Facile Synthesis of Single Crystal Vanadium Disulfide Nanosheets by Chemical Vapor Deposition for Efficient Hydrogen Evolution Reaction. Advanced Materials, 2015, 27, 5605-5609.	11.1	241
61	Novel Liquid Precursor-Based Facile Synthesis of Large-Area Continuous, Single, and Few-Layer Graphene Films. Chemistry of Materials, 2010, 22, 3457-3461.	3.2	239
62	Structure, Properties and Applications of Twoâ€Dimensional Hexagonal Boron Nitride. Advanced Materials, 2021, 33, e2101589.	11.1	239
63	Marine Corrosion Protective Coatings of Hexagonal Boron Nitride Thin Films on Stainless Steel. ACS Applied Materials & Interfaces, 2013, 5, 4129-4135.	4.0	234
64	Anomalous piezoelectricity in two-dimensional graphene nitride nanosheets. Nature Communications, 2014, 5, 4284.	5.8	228
65	Superior Potassium Ion Storage via Vertical MoS ₂ "Nanoâ€Rose―with Expanded Interlayers on Graphene. Small, 2017, 13, 1701471.	5.2	221
66	Binary and Ternary Atomic Layers Built from Carbon, Boron, and Nitrogen. Advanced Materials, 2012, 24, 4878-4895.	11.1	219
67	Boron- and Nitrogen-Substituted Graphene Nanoribbons as Efficient Catalysts for Oxygen Reduction Reaction. Chemistry of Materials, 2015, 27, 1181-1186.	3.2	219
68	Emerging Carbonâ€Based Heterogeneous Catalysts for Electrochemical Reduction of Carbon Dioxide into Valueâ€Added Chemicals. Advanced Materials, 2019, 31, e1804257.	11.1	218
69	Highâ€Lithiumâ€Affinity Chemically Exfoliated 2D Covalent Organic Frameworks. Advanced Materials, 2019, 31, e1901640.	11.1	217
70	Electrically Insulating Thermal Nano-Oils Using 2D Fillers. ACS Nano, 2012, 6, 1214-1220.	7.3	214
71	High thermal conductivity of suspended few-layer hexagonal boron nitride sheets. Nano Research, 2014, 7, 1232-1240.	5.8	211
72	Tracking Structural Selfâ€Reconstruction and Identifying True Active Sites toward Cobalt Oxychloride Precatalyst of Oxygen Evolution Reaction. Advanced Materials, 2019, 31, e1805127.	11.1	211

#	Article	IF	CITATIONS
73	Stable Metallic 1Tâ€WS ₂ Nanoribbons Intercalated with Ammonia Ions: The Correlation between Structure and Electrical/Optical Properties. Advanced Materials, 2015, 27, 4837-4844.	11.1	207
74	Nickel Vacancies Boost Reconstruction in Nickel Hydroxide Electrocatalyst. ACS Energy Letters, 2018, 3, 1373-1380.	8.8	206
75	A Scalable Approach to Dendriteâ€Free Lithium Anodes via Spontaneous Reduction of Sprayâ€Coated Graphene Oxide Layers. Advanced Materials, 2018, 30, e1801213.	11.1	204
76	Chemical Vapor Deposition of Monolayer Rhenium Disulfide (ReS ₂). Advanced Materials, 2015, 27, 4640-4648.	11.1	203
77	Electrical performance of monolayer MoS2 field-effect transistors prepared by chemical vapor deposition. Applied Physics Letters, 2013, 102, .	1.5	201
78	Recent developments of transition metal phosphides as catalysts in the energy conversionÂfield. Journal of Materials Chemistry A, 2018, 6, 23220-23243.	5.2	200
79	Temperature-dependent phonon shifts in monolayer MoS2. Applied Physics Letters, 2013, 103, .	1.5	199
80	Direct chemical conversion of graphene to boron- and nitrogen- and carbon-containing atomic layers. Nature Communications, 2014, 5, 3193.	5.8	198
81	Critical Role of Interface and Crystallinity on the Performance and Photostability of Perovskite Solar Cell on Nickel Oxide. Advanced Materials, 2018, 30, 1703879.	11.1	198
82	Surface functionalization of two-dimensional metal chalcogenides by Lewis acid–base chemistry. Nature Nanotechnology, 2016, 11, 465-471.	15.6	197
83	Re Doping in 2D Transition Metal Dichalcogenides as a New Route to Tailor Structural Phases and Induced Magnetism. Advanced Materials, 2017, 29, 1703754.	11.1	191
84	Atomic Cobalt Covalently Engineered Interlayers for Superior Lithiumâ€lon Storage. Advanced Materials, 2018, 30, e1802525.	11.1	187
85	Seawater electrolysis for hydrogen production: a solution looking for a problem?. Energy and Environmental Science, 2021, 14, 4831-4839.	15.6	187
86	Quaternary 2D Transition Metal Dichalcogenides (TMDs) with Tunable Bandgap. Advanced Materials, 2017, 29, 1702457.	11.1	186
87	Transforming Nickel Hydroxide into 3D Prussian Blue Analogue Array to Obtain Ni ₂ P/Fe ₂ P for Efficient Hydrogen Evolution Reaction. Advanced Energy Materials, 2018, 8, 1800484.	10.2	186
88	Electron Transfer Directed Antibacterial Properties of Graphene Oxide on Metals. Advanced Materials, 2018, 30, 1702149.	11.1	181
89	Mass and Charge Transfer Coenhanced Oxygen Evolution Behaviors in CoFeâ€Layered Double Hydroxide Assembled on Graphene. Advanced Materials Interfaces, 2016, 3, 1500782.	1.9	165
90	Rheniumâ€Doped and Stabilized MoS ₂ Atomic Layers with Basalâ€Plane Catalytic Activity. Advanced Materials, 2018, 30, e1803477.	11.1	164

#	Article	IF	CITATIONS
91	Formation of CuPd and CuPt Bimetallic Nanotubes by Galvanic Replacement Reaction. Journal of Physical Chemistry C, 2011, 115, 9403-9409.	1.5	163
92	Power from nature: designing green battery materials from electroactive quinone derivatives and organic polymers. Journal of Materials Chemistry A, 2016, 4, 12370-12386.	5.2	161
93	Lithium storage mechanisms in purpurin based organic lithium ion battery electrodes. Scientific Reports, 2012, 2, 960.	1.6	160
94	Carbon Nanotubeâ€Encapsulated Noble Metal Nanoparticle Hybrid as a Cathode Material for Liâ€Oxygen Batteries. Advanced Functional Materials, 2014, 24, 6516-6523.	7.8	157
95	Atomically thin gallium layers from solid-melt exfoliation. Science Advances, 2018, 4, e1701373.	4.7	157
96	Metallic 1T phase source/drain electrodes for field effect transistors from chemical vapor deposited MoS2. APL Materials, 2014, 2, .	2.2	155
97	Covalent Organic Frameworks for Batteries. Advanced Functional Materials, 2021, 31, 2100505.	7.8	154
98	High Strain Tolerant EMI Shielding Using Carbon Nanotube Network Stabilized Rubber Composite. Advanced Materials Technologies, 2017, 2, 1700078.	3.0	153
99	Design principles for electronic charge transport in solution-processed vertically stacked 2D perovskite quantum wells. Nature Communications, 2018, 9, 2130.	5.8	153
100	Synthesis of Millimeter cale Transition Metal Dichalcogenides Single Crystals. Advanced Functional Materials, 2016, 26, 2009-2015.	7.8	152
101	Wormâ€Shape Pt Nanocrystals Grown on Nitrogenâ€Doped Lowâ€Defect Graphene Sheets: Highly Efficient Electrocatalysts for Methanol Oxidation Reaction. Small, 2017, 13, 1603013.	5.2	151
102	Controlled synthesis of Mo-doped Ni ₃ S ₂ nano-rods: an efficient and stable electro-catalyst for water splitting. Journal of Materials Chemistry A, 2017, 5, 1595-1602.	5.2	148
103	Effect of H2O adsorption on electron transport in a carbon nanotube. Applied Physics Letters, 2002, 81, 2638-2640.	1.5	147
104	CoNi ₂ S ₄ â€Grapheneâ€2Dâ€MoSe ₂ as an Advanced Electrode Material for Supercapacitors. Advanced Energy Materials, 2016, 6, 1600341.	10.2	145
105	Conversion of non-van der Waals solids to 2D transition-metal chalcogenides. Nature, 2020, 577, 492-496.	13.7	145
106	Nanomechanical cleavage of molybdenum disulphide atomic layers. Nature Communications, 2014, 5, 3631.	5.8	144
107	Strong coupling and pressure engineering in WSe2–MoSe2 heterobilayers. Nature Physics, 2021, 17, 92-98.	6.5	140
108	Square selenene and tellurene: novel group VI elemental 2D materials with nontrivial topological properties. 2D Materials, 2017, 4, 041003.	2.0	139

#	Article	IF	CITATIONS
109	Brittle Fracture of 2D MoSe ₂ . Advanced Materials, 2017, 29, 1604201.	11.1	138
110	Exfoliated 2D Transition Metal Disulfides for Enhanced Electrocatalysis of Oxygen Evolution Reaction in Acidic Medium. Advanced Materials Interfaces, 2016, 3, 1500669.	1.9	136
111	Graphene–protein field effect biosensors: glucose sensing. Materials Today, 2015, 18, 513-522.	8.3	134
112	Controllable Codoping of Nitrogen and Sulfur in Graphene for Highly Efficient Li-Oxygen Batteries and Direct Methanol Fuel Cells. Chemistry of Materials, 2016, 28, 1737-1745.	3.2	132
113	Effect of Precursor Solution Aging on the Crystallinity and Photovoltaic Performance of Perovskite Solar Cells. Advanced Energy Materials, 2017, 7, 1602159.	10.2	130
114	Hexagonal Boron Nitride and Graphite Oxide Reinforced Multifunctional Porous Cement Composites. Advanced Functional Materials, 2013, 23, 5624-5630.	7.8	129
115	Three-dimensional mesostructures as high-temperature growth templates, electronic cellular scaffolds, and self-propelled microrobots. Proceedings of the National Academy of Sciences of the United States of America, 2017, 114, E9455-E9464.	3.3	129
116	Gold Nanoparticles and g ₃ N ₄ â€intercalated Graphene Oxide Membrane for Recyclable Surface Enhanced Raman Scattering. Advanced Functional Materials, 2017, 27, 1701714.	7.8	129
117	How Nitrogen-Doped Graphene Quantum Dots Catalyze Electroreduction of CO ₂ to Hydrocarbons and Oxygenates. ACS Catalysis, 2017, 7, 6245-6250.	5.5	129
118	Surface Tension Components Based Selection of Cosolvents for Efficient Liquid Phase Exfoliation of 2D Materials. Small, 2016, 12, 2741-2749.	5.2	128
119	Synthesis of large-scale atomic-layer SnS2 through chemical vapor deposition. Nano Research, 2017, 10, 2386-2394.	5.8	124
120	Imaging the motion of electrons across semiconductor heterojunctions. Nature Nanotechnology, 2017, 12, 36-40.	15.6	124
121	Improving the Catalytic Activity of Carbon‣upported Single Atom Catalysts by Polynary Metal or Heteroatom Doping. Small, 2020, 16, e1906782.	5.2	124
122	Tellurium-Assisted Low-Temperature Synthesis of MoS ₂ and WS ₂ Monolayers. ACS Nano, 2015, 9, 11658-11666.	7.3	123
123	Strain-Induced Electronic Structure Changes in Stacked van der Waals Heterostructures. Nano Letters, 2016, 16, 3314-3320.	4.5	122
124	Fluorinated h-BN as a magnetic semiconductor. Science Advances, 2017, 3, e1700842.	4.7	121
125	Highly Inâ€Plane Optical and Electrical Anisotropy of 2D Germanium Arsenide. Advanced Functional Materials, 2018, 28, 1707379.	7.8	121
126	Boron Nitride–Graphene Nanocapacitor and the Origins of Anomalous Size-Dependent Increase of Capacitance. Nano Letters, 2014, 14, 1739-1744.	4.5	120

#	Article	IF	CITATIONS
127	Carbon Nitrogen Nanotubes as Efficient Bifunctional Electrocatalysts for Oxygen Reduction and Evolution Reactions. ACS Applied Materials & Interfaces, 2015, 7, 11991-12000.	4.0	120
128	Characterizing energy dissipation in single-walled carbon nanotube polycarbonate composites. Applied Physics Letters, 2005, 87, 063102.	1.5	119
129	Spectroscopic Signatures of AA′ and AB Stacking of Chemical Vapor Deposited Bilayer MoS ₂ . ACS Nano, 2015, 9, 12246-12254.	7.3	117
130	Etchingâ€Doping Sedimentation Equilibrium Strategy: Accelerating Kinetics on Hollow Rhâ€Doped CoFeâ€Layered Double Hydroxides for Water Splitting. Advanced Functional Materials, 2020, 30, 2003556.	7.8	117
131	Controlled Electrodeposition Synthesis of Co–Ni–P Film as a Flexible and Inexpensive Electrode for Efficient Overall Water Splitting. ACS Applied Materials & Interfaces, 2017, 9, 31887-31896.	4.0	116
132	Probing the phonon dispersion relations of graphite from the double-resonance process of Stokes and anti-Stokes Raman scatterings in multiwalled carbon nanotubes. Physical Review B, 2002, 66, .	1.1	113
133	Hexagonal Boron Nitrideâ€Based Electrolyte Composite for Liâ€ l on Battery Operation from Room Temperature to 150 °C. Advanced Energy Materials, 2016, 6, 1600218.	10.2	112
134	Fatigue of graphene. Nature Materials, 2020, 19, 405-411.	13.3	110
135	Metal-Oxide-Mediated Subtractive Manufacturing of Two-Dimensional Carbon Nitride for High-Efficiency and High-Yield Photocatalytic H ₂ Evolution. ACS Nano, 2019, 13, 11294-11302.	7.3	109
136	Tuning the Electrochemical Reactivity of Boron―and Nitrogen‧ubstituted Graphene. Advanced Materials, 2016, 28, 6239-6246.	11.1	107
137	Graphene Supported MoS ₂ Structures with High Defect Density for an Efficient HER Electrocatalysts. ACS Applied Materials & Interfaces, 2020, 12, 12629-12638.	4.0	101
138	Pronounced Photovoltaic Response from Multilayered Transition-Metal Dichalcogenides PN-Junctions. Nano Letters, 2015, 15, 7532-7538.	4.5	98
139	Multifunctional Bioâ€Nanocomposite Coatings for Perishable Fruits. Advanced Materials, 2020, 32, e1908291.	11.1	97
140	Growth-substrate induced performance degradation in chemically synthesized monolayer MoS2 field effect transistors. Applied Physics Letters, 2014, 104, .	1.5	96
141	Correlating the three-dimensional atomic defects and electronic properties of two-dimensional transition metal dichalcogenides. Nature Materials, 2020, 19, 867-873.	13.3	96
142	Atomic Ru Immobilized on Porous h-BN through Simple Vacuum Filtration for Highly Active and Selective CO ₂ Methanation. ACS Catalysis, 2019, 9, 10077-10086.	5.5	93
143	A solvent-assisted ligand exchange approach enables metal-organic frameworks with diverse and complex architectures. Nature Communications, 2020, 11, 927.	5.8	93
144	3D-printed silica with nanoscale resolution. Nature Materials, 2021, 20, 1506-1511.	13.3	93

#	Article	IF	CITATIONS
145	Sustainable Synthesis of Bright Green Fluorescent Nitrogenâ€Doped Carbon Quantum Dots from Alkali Lignin. ChemSusChem, 2019, 12, 4202-4210.	3.6	92
146	Low-density three-dimensional foam using self-reinforced hybrid two-dimensional atomic layers. Nature Communications, 2014, 5, 4541.	5.8	91
147	Cryo-mediated exfoliation and fracturing of layered materials into 2D quantum dots. Science Advances, 2017, 3, e1701500.	4.7	91
148	Ni filled flexible multi-walled carbon nanotube–polystyrene composite films as efficient microwave absorbers. Applied Physics Letters, 2011, 99, .	1.5	90
149	Reversible Formation of g ₃ N ₄ 3D Hydrogels through Ionic Liquid Activation: Gelation Behavior and Roomâ€Temperature Gasâ€Sensing Properties. Advanced Functional Materials, 2017, 27, 1700653.	7.8	90
150	Regulation of functional groups on graphene quantum dots directs selective CO2 to CH4 conversion. Nature Communications, 2021, 12, 5265.	5.8	89
151	Utilizing interfaces in carbon nanotube reinforced polymer composites for structural damping. Journal of Materials Science, 2006, 41, 7824-7829.	1.7	88
152	Multifunctional nanocoated membranes for high-rate electrothermal desalination of hypersaline waters. Nature Nanotechnology, 2020, 15, 1025-1032.	15.6	88
153	Temperature dependent electrical transport of disordered reduced graphene oxide. 2D Materials, 2014, 1, 011008.	2.0	86
154	Manipulation on active electronic states of metastable phase β-NiMoO4 for large current density hydrogen evolution. Nature Communications, 2021, 12, 5960.	5.8	86
155	2D TiS ₂ Layers: A Superior Nonlinear Optical Limiting Material. Advanced Optical Materials, 2017, 5, 1700713.	3.6	84
156	Super-elasticity of three-dimensionally cross-linked graphene materials all the way to deep cryogenic temperatures. Science Advances, 2019, 5, eaav2589.	4.7	84
157	A Non-van der Waals Two-Dimensional Material from Natural Titanium Mineral Ore Ilmenite. Chemistry of Materials, 2018, 30, 5923-5931.	3.2	82
158	Synthesis of Low-Density, Carbon-Doped, Porous Hexagonal Boron Nitride Solids. ACS Nano, 2015, 9, 12088-12095.	7.3	81
159	HClâ€Based Hydrothermal Etching Strategy toward Fluorideâ€Free MXenes. Advanced Materials, 2021, 33, e2101015.	11.1	79
160	Alloyed 2D Metal–Semiconductor Atomic Layer Junctions. Nano Letters, 2016, 16, 1890-1895.	4.5	77
161	Electromechanically Responsive Liquid Crystal Elastomer Nanocomposites for Active Cell Culture. ACS Macro Letters, 2016, 5, 1386-1390.	2.3	76
162	Synthesis of Highâ€Quality Graphene and Hexagonal Boron Nitride Monolayer Inâ€Plane Heterostructure on Cu–Ni Alloy. Advanced Science, 2017, 4, 1700076.	5.6	76

#	Article	IF	CITATIONS
163	Multiscale Geometric Design Principles Applied to 3D Printed Schwarzites. Advanced Materials, 2018, 30, 1704820.	11.1	76
164	Localized Ostwald Ripening Guided Dissolution/Regrowth to Ancient Chinese Coinâ€shaped VO ₂ Nanoplates with Enhanced Mass Transfer for Zinc Ion Storage. Advanced Functional Materials, 2020, 30, 2000472.	7.8	76
165	Aligned Carbon Nanotube Stationary Phases for Electrochromatographic Chip Separations. Chromatographia, 2009, 69, 473-480.	0.7	72
166	Super-elasticity at 4 K of covalently crosslinked polyimide aerogels with negative Poisson's ratio. Nature Communications, 2021, 12, 4092.	5.8	72
167	Carbon Dioxide Hydrogenation over a Metal-Free Carbon-Based Catalyst. ACS Catalysis, 2017, 7, 4497-4503.	5.5	71
168	Observation of Dynamic Strain Hardening in Polymer Nanocomposites. ACS Nano, 2011, 5, 2715-2722.	7.3	70
169	Low Contact Barrier in 2H/1T′ MoTe ₂ In-Plane Heterostructure Synthesized by Chemical Vapor Deposition. ACS Applied Materials & Interfaces, 2019, 11, 12777-12785.	4.0	70
170	Active Control of Plasmon–Exciton Coupling in MoS ₂ –Ag Hybrid Nanostructures. Advanced Optical Materials, 2016, 4, 1463-1469.	3.6	69
171	Experimental Determination of the Ionization Energies of MoSe ₂ , WS ₂ , and MoS ₂ on SiO ₂ Using Photoemission Electron Microscopy. ACS Nano, 2017, 11, 8223-8230.	7.3	69
172	Doping Nanoscale Graphene Domains Improves Magnetism in Hexagonal Boron Nitride. Advanced Materials, 2019, 31, e1805778.	11.1	69
173	Integrated Energy Aerogel of N,S-rGO/WSe ₂ /NiFe-LDH for Both Energy Conversion and Storage. ACS Applied Materials & Interfaces, 2017, 9, 32756-32766.	4.0	68
174	Polytypism in ultrathin tellurium. 2D Materials, 2019, 6, 015013.	2.0	68
175	Controlled Synthesis of Eutectic NiSe/Ni ₃ Se ₂ Self‣upported on Ni Foam: An Excellent Bifunctional Electrocatalyst for Overall Water Splitting. Advanced Materials Interfaces, 2018, 5, 1701507.	1.9	67
176	Spontaneous self-intercalation of copper atoms into transition metal dichalcogenides. Science Advances, 2020, 6, eaay4092.	4.7	67
177	Charge-injection-induced dynamic screening and origin of hysteresis in field-modulated transport in single-wall carbon nanotubes. Applied Physics Letters, 2006, 89, 162108.	1.5	65
178	Transforming collagen wastes into doped nanocarbons for sustainable energy applications. Green Chemistry, 2012, 14, 1689.	4.6	65
179	Tunable Electronics in Large-Area Atomic Layers of Boron–Nitrogen–Carbon. Nano Letters, 2013, 13, 3476-3481.	4.5	65
180	Designing nanoscaled hybrids from atomic layered boron nitride with silver nanoparticle deposition. Journal of Materials Chemistry A, 2014, 2, 3148.	5.2	65

#	Article	IF	CITATIONS
181	Fiber Reinforced Layered Dielectric Nanocomposite. Advanced Functional Materials, 2019, 29, 1900056.	7.8	64
182	Layer Engineering of 2D Semiconductor Junctions. Advanced Materials, 2016, 28, 5126-5132.	11.1	63
183	In Situ Synthesis of Lead-Free Halide Perovskite–COF Nanocomposites as Photocatalysts for Photoinduced Polymerization in Both Organic and Aqueous Phases. , 2022, 4, 464-471.		63
184	Adsorption energy of oxygen molecules on graphene and two-dimensional tungsten disulfide. Scientific Reports, 2017, 7, 1774.	1.6	62
185	Pure Crystalline Covalent Organic Framework Aerogels. Chemistry of Materials, 2021, 33, 4216-4224.	3.2	62
186	Facile Green Synthesis of BCN Nanosheets as Highâ€Performance Electrode Material for Electrochemical Energy Storage. Chemistry - A European Journal, 2016, 22, 7134-7140.	1.7	61
187	Highly versatile SPION encapsulated PLGA nanoparticles as photothermal ablators of cancer cells and as multimodal imaging agents. Biomaterials Science, 2017, 5, 432-443.	2.6	61
188	Metal Immiscibility Route to Synthesis of Ultrathin Carbides, Borides, and Nitrides. Advanced Materials, 2017, 29, 1700364.	11.1	61
189	Revisiting the Role of Active Sites for Hydrogen Evolution Reaction through Precise Defect Adjusting. Advanced Functional Materials, 2019, 29, 1901290.	7.8	61
190	An <i>in situ</i> electrochemical oxidation strategy for formation of nanogrid-shaped V ₃ O ₇ ·H ₂ O with enhanced zinc storage properties. Journal of Materials Chemistry A, 2019, 7, 25262-25267.	5.2	61
191	Reactive 3D Printing of Shape-Programmable Liquid Crystal Elastomer Actuators. ACS Applied Materials & Interfaces, 2020, 12, 28692-28699.	4.0	61
192	Selfâ€Assembled Fullerene Nanostructures: Synthesis and Applications. Advanced Functional Materials, 2022, 32, 2106924.	7.8	61
193	Nanosized Pt anchored onto 3D nitrogen-doped graphene nanoribbons towards efficient methanol electrooxidation. Journal of Materials Chemistry A, 2015, 3, 19696-19701.	5.2	60
194	Amineâ€Functionalized Carbon Nanodot Electrocatalysts Converting Carbon Dioxide to Methane. Advanced Materials, 2022, 34, e2105690.	11.1	59
195	Structural Phase Transformation in Strained Monolayer MoWSe ₂ Alloy. ACS Nano, 2018, 12, 3468-3476.	7.3	57
196	Light-Assisted Rechargeable Lithium Batteries: Organic Molecules for Simultaneous Energy Harvesting and Storage. Nano Letters, 2021, 21, 907-913.	4.5	57
197	Manganese buffer induced high-performance disordered MnVO cathodes in zinc batteries. Energy and Environmental Science, 2021, 14, 3954-3964.	15.6	57
198	Liquid metal-tailored gluten network for protein-based e-skin. Nature Communications, 2022, 13, 1206.	5.8	57

#	Article	IF	CITATIONS
199	Hexagonal Boron Nitride for Sulfur Corrosion Inhibition. ACS Nano, 2020, 14, 14809-14819.	7.3	56
200	Spiral Growth of SnSe ₂ Crystals by Chemical Vapor Deposition. Advanced Materials Interfaces, 2016, 3, 1600383.	1.9	55
201	Quasi-Solid Electrolytes for High Temperature Lithium Ion Batteries. ACS Applied Materials & Interfaces, 2015, 7, 25777-25783.	4.0	54
202	Deformation Mechanisms of Vertically Stacked WS ₂ /MoS ₂ Heterostructures: The Role of Interfaces. ACS Nano, 2018, 12, 4036-4044.	7.3	54
203	Quantitative analysis of hysteresis in carbon nanotube field-effect devices. Applied Physics Letters, 2006, 89, 132118.	1.5	53
204	2D Crystals Significantly Enhance the Performance of a Working Fuel Cell. Advanced Energy Materials, 2017, 7, 1601216.	10.2	53
205	Sublimationâ€Vapor Phase Pseudomorphic Transformation of Templateâ€Directed MOFs for Efficient Oxygen Evolution Reaction. Advanced Functional Materials, 2019, 29, 1903875.	7.8	53
206	Spectral fingerprinting of structural defects in plasma-treated carbon nanotubes. Journal of Materials Research, 2003, 18, 2515-2521.	1.2	52
207	3D Porous Graphene by Lowâ€Temperature Plasma Welding for Bone Implants. Advanced Materials, 2016, 28, 8959-8967.	11.1	52
208	Ultrafast non-radiative dynamics of atomically thin MoSe2. Nature Communications, 2017, 8, 1745.	5.8	52
209	Oxidizing Vacancies in Nitrogenâ€Doped Carbon Enhance Airâ€Cathode Activity. Advanced Materials, 2019, 31, e1803339.	11.1	52
210	Ionic Liquid–Organic Carbonate Electrolyte Blends To Stabilize Silicon Electrodes for Extending Lithium Ion Battery Operability to 100 °C. ACS Applied Materials & Interfaces, 2016, 8, 15242-15249.	4.0	51
211	2D Electrets of Ultrathin MoO ₂ with Apparent Piezoelectricity. Advanced Materials, 2020, 32, e2000006.	11.1	51
212	Water-Soluble Defect-Rich MoS ₂ Ultrathin Nanosheets for Enhanced Hydrogen Evolution. Journal of Physical Chemistry Letters, 2019, 10, 3282-3289.	2.1	50
213	Lateral Monolayer MoSe ₂ –WSe ₂ p–n Heterojunctions with Giant Builtâ€in Potentials. Small, 2020, 16, e2002263.	5.2	50
214	3D Reduced Graphene Oxide Coated V ₂ O ₅ Nanoribbon Scaffolds for High-Capacity Supercapacitor Electrodes. Particle and Particle Systems Characterization, 2015, 32, 817-821.	1.2	49
215	Morphogenesis and mechanostabilization of complex natural and 3D printed shapes. Science Advances, 2015, 1, e1400052.	4.7	48
216	Multifunctional Cu2â^'xTe Nanocubes Mediated Combination Therapy for Multi-Drug Resistant MDA MB 453. Scientific Reports, 2016, 6, 35961.	1.6	48

#	Article	IF	CITATIONS
217	Dynamic Hosts for High-Performance Li–S Batteries Studied by Cryogenic Transmission Electron Microscopy and in Situ X-ray Diffraction. ACS Energy Letters, 2018, 3, 1325-1330.	8.8	47
218	Recyclable three-dimensional Ag nanorod arrays decorated with O-g-C3N4 for highly sensitive SERS sensing of organic pollutants. Journal of Hazardous Materials, 2019, 379, 120823.	6.5	47
219	Rational Design of Oxygen-Enriched Carbon Dots with Efficient Room-Temperature Phosphorescent Properties and High-Tech Security Protection Application. ACS Sustainable Chemistry and Engineering, 2019, 7, 19918-19924.	3.2	47
220	High hardness in the biocompatible intermetallic compound β-Ti ₃ Au. Science Advances, 2016, 2, e1600319.	4.7	46
221	MoS ₂ –Carbon Nanotube Porous 3 D Network for Enhanced Oxygen Reduction Reaction. ChemSusChem, 2018, 11, 2960-2966.	3.6	46
222	Structural Defects Modulate Electronic and Nanomechanical Properties of 2D Materials. ACS Nano, 2021, 15, 2520-2531.	7.3	46
223	Thermal resistance of the native interface between vertically aligned multiwalled carbon nanotube arrays and their SiO2/Si substrate. Journal of Applied Physics, 2008, 103, .	1.1	45
224	Surface Tension Components Ratio: An Efficient Parameter for Direct Liquid Phase Exfoliation. ACS Applied Materials & Interfaces, 2017, 9, 9168-9175.	4.0	45
225	<i>In Situ</i> Synthesis of Metal Nanoparticle Embedded Hybrid Soft Nanomaterials. Accounts of Chemical Research, 2016, 49, 1671-1680.	7.6	44
226	Ternary Culn ₇ Se ₁₁ : Towards Ultraâ€Thin Layered Photodetectors and Photovoltaic Devices. Advanced Materials, 2014, 26, 7666-7672.	11.1	43
227	Valley trion dynamics in monolayer <mml:math xmlns:mml="http://www.w3.org/1998/Math/MathML"><mml:msub><mml:mi>MoSe</mml:mi><mml:mn>2Physical Review B, 2016, 94, .</mml:mn></mml:msub></mml:math 	il:mun.> <td>ml#masub></td>	ml#masub>
228	Novel FeNi ₂ S ₄ /TMD-based ternary composites for supercapacitor applications. Journal of Materials Chemistry A, 2016, 4, 8844-8850.	5.2	43
229	Phonon-Suppressed Auger Scattering of Charge Carriers in Defective Two-Dimensional Transition Metal Dichalcogenides. Nano Letters, 2019, 19, 6078-6086.	4.5	43
230	Anomalous insulator-metal transition in boron nitride-graphene hybrid atomic layers. Physical Review B, 2012, 86, .	1.1	42
231	Observing the interplay between surface and bulk optical nonlinearities in thin van der Waals crystals. Scientific Reports, 2016, 6, 22620.	1.6	42
232	Defect-Mediated Alloying of Monolayer Transition-Metal Dichalcogenides. ACS Nano, 2018, 12, 12795-12804.	7.3	42
233	Low-Cost, Large-Area, Facile, and Rapid Fabrication of Aligned ZnO Nanowire Device Arrays. ACS Applied Materials & Interfaces, 2016, 8, 13466-13471.	4.0	41
234	Covalently Connected Carbon Nanotubes as Electrocatalysts for Hydrogen Evolution Reaction through Band Engineering. ACS Catalysis, 2017, 7, 2676-2684.	5.5	41

#	Article	IF	CITATIONS
235	Controlled Ohmic and nonlinear electrical transport in inkjet-printed single-wall carbon nanotube films. Physical Review B, 2008, 77, .	1.1	40
236	Terahertz Characterization of Single-Walled Carbon Nanotube and Graphene On-Substrate Thin Films. IEEE Transactions on Microwave Theory and Techniques, 2011, 59, 2719-2725.	2.9	40
237	Long-term behavior of epoxy/graphene-based composites determined by dynamic mechanical analysis. Journal of Materials Science, 2015, 50, 6407-6419.	1.7	40
238	Interphase Induced Dynamic Selfâ€ S tiffening in Grapheneâ€Based Polydimethylsiloxane Nanocomposites. Small, 2016, 12, 3723-3731.	5.2	39
239	All-Carbon Ultrafast Supercapacitor by Integrating Multidimensional Nanocarbons. Small, 2016, 12, 5684-5691.	5.2	39
240	Effect of Carrier Localization on Electrical Transport and Noise at Individual Grain Boundaries in Monolayer MoS ₂ . Nano Letters, 2017, 17, 5452-5457.	4.5	39
241	Self-assembled large scale metal alloy grid patterns as flexible transparent conductive layers. Scientific Reports, 2015, 5, 13710.	1.6	38
242	Scalable Transfer of Suspended Two-Dimensional Single Crystals. Nano Letters, 2015, 15, 5089-5097.	4.5	38
243	Simultaneous Observation of Carrier-Specific Redistribution and Coherent Lattice Dynamics in 2H-MoTe ₂ with Femtosecond Core-Level Spectroscopy. ACS Nano, 2020, 14, 15829-15840. Blueshift of the <mml:math <="" td="" xmlns:mml="http://www.w3.org/1998/Math/MathML"><td>7.3</td><td>38</td></mml:math>	7.3	38
244	display="inline"> <mml:mi>A</mml:mi> -excition peak in folded monolayer <mml:math xmlns:mml="http://www.w3.org/1998/Math/MathML" display="inline"><mml:mrow><mml:mn>1</mml:mn><mml:mi>H</mml:mi></mml:mrow>-MoS<mr xmlns:mml="http://www.w3.org/1998/Math/MathML" display="inline"><mml:msub><mml:mrow>-MoS<mr< td=""><td>nl:math</td><td>37</td></mr<></mml:mrow></mml:msub></mr </mml:math 	nl:math	37
245	/> <mml:mn>2</mml:mn> . Physical Review B, 2013, 88, . Telluride-Based Atomically Thin Layers of Ternary Two-Dimensional Transition Metal Dichalcogenide Alloys. Chemistry of Materials, 2018, 30, 7262-7268.	3.2	37
246	Carbon nanocoils for multi-functional energy applications. Journal of Materials Chemistry, 2011, 21, 16103.	6.7	36
247	Strain Rate Dependent Shear Plasticity in Graphite Oxide. Nano Letters, 2016, 16, 1127-1131.	4.5	36
248	Chromiteen: A New 2D Oxide Magnetic Material from Natural Ore. Advanced Materials Interfaces, 2018, 5, 1800549.	1.9	36
249	Made From Henna! A Fast-Charging, High-Capacity, and Recyclable Tetrakislawsone Cathode Material for Lithium Ion Batteries. ACS Sustainable Chemistry and Engineering, 2019, 7, 13836-13844.	3.2	36
250	A Low-Cost and High-Efficiency Integrated Device toward Solar-Driven Water Splitting. ACS Nano, 2020, 14, 5426-5434.	7.3	36
251	Massive Icosahedral Boron Carbide Crystals. Journal of Physical Chemistry B, 2002, 106, 5807-5809.	1.2	35
252	Ambient solid-state mechano-chemical reactions between functionalized carbon nanotubes. Nature Communications, 2015, 6, 7291.	5.8	35

#	Article	IF	CITATIONS
253	Ultrafast Optical Microscopy of Single Monolayer Molybdenum Disulfide Flakes. Scientific Reports, 2016, 6, 21601 Layer dependence of the electronic band alignment of few-layer <mml:math xmlns:mml="http://www.w3.org/1998/Math/MathML"><mml:mrow><mml:mi>Mo</mml:mi><mml:msub><mml:m< td=""><td>1.6 i</td><td>35</td></mml:m<></mml:msub></mml:mrow></mml:math 	1.6 i	35
254	mathvariant="normal">S <mml:mn>2</mml:mn> on <mml:math xmlns:mml="http://www.w3.org/1998/Math/MathML"><mml:mrow><mml:mi>Si</mml:mi><mml:msub>mathvariant="normal">O<mml:mn>2</mml:mn></mml:msub></mml:mrow></mml:math 	1.1	35
255	Nonlinear Dark-Field Imaging of One-Dimensional Defects in Monolayer Dichalcogenides. Nano Letters, 2020, 20, 284-291.	4.5	34
256	Zn ²⁺ -Intercalated V ₂ O ₅ · <i>n</i> H ₂ O derived from V ₂ CT _{<i>x</i>} MXene for hyper-stable zinc-ion storage. Journal of Materials Chemistry A, 2021, 9, 17994-18005.	5.2	34
257	A common tattoo chemical for energy storage: henna plant-derived naphthoquinone dimer as a green and sustainable cathode material for Li-ion batteries. RSC Advances, 2018, 8, 1576-1582.	1.7	33
258	Magnetic Properties and Photocatalytic Applications of 2D Sheets of Nonlayered Manganese Telluride by Liquid Exfoliation. ACS Applied Nano Materials, 2018, 1, 6427-6434.	2.4	33
259	Ionically Self-Assembled Polyelectrolyte-Based Carbon Nanotube Fibers. Chemistry of Materials, 2009, 21, 3062-3071.	3.2	32
260	Bioderived Molecular Electrodes for Nextâ€Generation Energyâ€Storage Materials. ChemSusChem, 2020, 13, 2186-2204.	3.6	32
261	Damage-tolerant 3D-printed ceramics via conformal coating. Science Advances, 2021, 7, .	4.7	32
262	Aquaporin–graphene interface: relevance to point-of-care device for renal cell carcinoma and desalination. Interface Focus, 2018, 8, 20170066.	1.5	31
263	Urchin-like CoP with Controlled Manganese Doping toward Efficient Hydrogen Evolution Reaction in Both Acid and Alkaline Solution. ACS Sustainable Chemistry and Engineering, 2018, 6, 15162-15169.	3.2	31
264	Designing a sustainable fluorescent targeting probe for superselective nucleus imaging. Carbon, 2021, 180, 48-55.	5.4	31
265	Nature Inspired Strategy to Enhance Mechanical Properties via Liquid Reinforcement. Advanced Materials Interfaces, 2017, 4, 1700240.	1.9	30
266	Atomic Layered Titanium Sulfide Quantum Dots as Electrocatalysts for Enhanced Hydrogen Evolution Reaction. Advanced Materials Interfaces, 2018, 5, 1700895.	1.9	30
267	Ultrafast probes of electron–hole transitions between two atomic layers. Nature Communications, 2018, 9, 1859.	5.8	30
268	Two-Dimensional Lateral Epitaxy of 2H (MoSe ₂)–1T′ (ReSe ₂) Phases. Nano Letters, 2019, 19, 6338-6345.	4.5	30
269	Interface and defect engineering of hybrid nanostructures toward an efficient HER catalyst. Nanoscale, 2019, 11, 12489-12496.	2.8	30
270	Free-standing SnS/carbonized cellulose film as durable anode for lithium-ion batteries. Carbohydrate Polymers, 2021, 255, 117400.	5.1	30

#	Article	IF	CITATIONS
271	Apparent Ferromagnetism in Exfoliated Ultrathin Pyrite Sheets. Journal of Physical Chemistry C, 2021, 125, 18927-18935.	1.5	30
272	Three-Dimensional Porous Sponges from Collagen Biowastes. ACS Applied Materials & Interfaces, 2016, 8, 14836-14844.	4.0	29
273	Enhanced thermal conductivity and mechanical properties of hybrid MoS ₂ /hâ€BN polyurethane nanocomposites. Journal of Applied Polymer Science, 2018, 135, 46560.	1.3	29
274	Thermally Induced 2D Alloyâ€Heterostructure Transformation in Quaternary Alloys. Advanced Materials, 2018, 30, e1804218.	11.1	29
275	Facile synthesis of highly fluorescent free-standing films comprising graphitic carbon nitride (g-C ₃ N ₄) nanolayers. New Journal of Chemistry, 2020, 44, 2644-2651.	1.4	29
276	3Dâ€Bioprinted Inflammation Modulating Polymer Scaffolds for Soft Tissue Repair. Advanced Materials, 2021, 33, e2003778.	11.1	29
277	Label-free as-grown double wall carbon nanotubes bundles for Salmonella typhimuriumimmunoassay. Chemistry Central Journal, 2013, 7, 102.	2.6	28
278	Giant quasiparticle bandgap modulation in graphene nanoribbons supported on weakly interacting surfaces. Applied Physics Letters, 2013, 103, .	1.5	28
279	Zirconiaâ€Nanoparticleâ€Reinforced Morphologyâ€Engineered Grapheneâ€Based Foams. Advanced Materials, 2015, 27, 4534-4543.	11.1	28
280	Layer-by-layer self-assembly of polyelectrolyte functionalized MoS ₂ nanosheets. Nanoscale, 2016, 8, 9641-9647.	2.8	28
281	Nanotechnology Research and Development in Upstream Oil and Gas. Energy Technology, 2020, 8, 1901216.	1.8	28
282	Solid–Vapor Reaction Growth of Transitionâ€Metal Dichalcogenide Monolayers. Angewandte Chemie - International Edition, 2016, 55, 10656-10661.	7.2	27
283	Phase Segregation Behavior of Two-Dimensional Transition Metal Dichalcogenide Binary Alloys Induced by Dissimilar Substitution. Chemistry of Materials, 2017, 29, 7431-7439.	3.2	27
284	Optical Control of Non-Equilibrium Phonon Dynamics. Nano Letters, 2019, 19, 4981-4989.	4.5	27
285	The modulating effect of N coordination on single-atom catalysts researched by Pt-N -C model through both experimental study and DFT simulation. Journal of Materials Science and Technology, 2021, 91, 160-167.	5.6	27
286	Nanoscale-Barrier Formation Induced by Low-Dose Electron-Beam Exposure in Ultrathin MoS ₂ Transistors. ACS Nano, 2016, 10, 9730-9737.	7.3	26
287	An Insight into the Phase Transformation of WS ₂ upon Fluorination. Advanced Materials, 2018, 30, e1803366.	11.1	26
288	Template-free solvothermal preparation of ternary FeNi ₂ S ₄ hollow balloons as RuO ₂ -like efficient electrocatalysts for the oxygen evolution reaction with superior stability. Journal of Materials Chemistry A, 2018, 6, 19417-19424.	5.2	26

#	Article	IF	CITATIONS
289	Liâ€Breathing Air Batteries Catalyzed by MnNiFe/Laserâ€Induced Graphene Catalysts. Advanced Materials Interfaces, 2019, 6, 1901035.	1.9	26
290	Rapid, Ambient Temperature Synthesis of Imine Covalent Organic Frameworks Catalyzed by Transition-Metal Nitrates. Chemistry of Materials, 2021, 33, 3394-3400.	3.2	26
291	Additive manufacturing of polymer-based structures by extrusion technologies. Oxford Open Materials Science, 2020, 1, .	0.5	26
292	Controlled 3D Carbon Nanotube Structures by Plasma Welding. Advanced Materials Interfaces, 2016, 3, 1500755.	1.9	25
293	Metalâ€Free Dual Modal Contrast Agents Based on Fluorographene Quantum Dots. Particle and Particle Systems Characterization, 2017, 34, 1600221.	1.2	25
294	Precursorâ€Transformation Strategy Preparation of CuP x Nanodots–Decorated CoP 3 Nanowires Hybrid Catalysts for Boosting pHâ€Universal Electrocatalytic Hydrogen Evolution. Small, 2019, 15, 1904681.	5.2	25
295	Sustainable Synthesis of Nâ€Doped Hollow Porous Carbon Spheres via a Sprayâ€Drying Method for Lithiumâ€Sulfur Storage with Ultralong Cycle Life. Batteries and Supercaps, 2020, 3, 1201-1208.	2.4	25
296	FIBâ€Patterned Nano‣upercapacitors: Minimized Size with Ultrahigh Performances. Advanced Materials, 2020, 32, e1908072.	11.1	25
297	Metal Oxide Catalysts for the Synthesis of Covalent Organic Frameworks and One-Step Preparation of Covalent Organic Framework-Based Composites. Chemistry of Materials, 2021, 33, 6158-6165.	3.2	25
298	Transformation of One-Dimensional Linear Polymers into Two-Dimensional Covalent Organic Frameworks Through Sequential Reversible and Irreversible Chemistries. Chemistry of Materials, 2021, 33, 413-419.	3.2	25
299	Photo Rechargeable Li″on Batteries Using Nanorod Heterostructure Electrodes. Small, 2021, 17, e2105029.	5.2	25
300	Velcro-Inspired SiC Fuzzy Fibers for Aerospace Applications. ACS Applied Materials & Interfaces, 2017, 9, 13742-13750.	4.0	24
301	Fast photoresponse and high detectivity in copper indium selenide (CuIn 7 Se 11) phototransistors. 2D Materials, 2018, 5, 015001.	2.0	24
302	Synthesis and 3D Interconnected Nanostructured h-BN-Based Biocomposites by Low-Temperature Plasma Sintering: Bone Regeneration Applications. ACS Omega, 2018, 3, 6013-6021.	1.6	24
303	3D Printed Tubulanes as Lightweight Hypervelocity Impact Resistant Structures. Small, 2019, 15, e1904747.	5.2	24
304	Synthetic Engineering of Morphology and Electronic Band Gap in Lateral Heterostructures of Monolayer Transition Metal Dichalcogenides. ACS Nano, 2020, 14, 6323-6330.	7.3	24
305	Graphene-incorporated aluminum with enhanced thermal and mechanical properties for solar heat collectors. AIP Advances, 2020, 10, .	0.6	24
306	Self-assembly of 0D/2D homostructure for enhanced hydrogen evolution. Materials Today, 2020, 36, 83-90.	8.3	24

#	Article	IF	CITATIONS
307	Achieving Highâ€Quality Freshwater from a Selfâ€&ustainable Integrated Solar Redoxâ€Flow Desalination Device. Small, 2021, 17, e2100490.	5.2	24
308	Inkjet printed resistive and chemicalâ€FET carbon nanotube gas sensors. Physica Status Solidi (B): Basic Research, 2008, 245, 2335-2338.	0.7	23
309	Fluctuation-Enhanced Sensing: Status and Perspectives. IEEE Sensors Journal, 2008, 8, 714-719.	2.4	23
310	Electromechanical Properties of Polymer Electrolyteâ€Based Stretchable Supercapacitors. Advanced Energy Materials, 2014, 4, 1300844.	10.2	23
311	Large-scale controlled synthesis of porous two-dimensional nanosheets for the hydrogen evolution reaction through a chemical pathway. Nanoscale, 2018, 10, 6168-6176.	2.8	23
312	Strain relaxation via formation of cracks in compositionally modulated two-dimensional semiconductor alloys. Npj 2D Materials and Applications, 2018, 2, .	3.9	23
313	Nb ₂ O ₅ /reduced Graphene Oxide Nanocomposite Anode for High Power Hybrid Supercapacitor Applications. ChemistrySelect, 2019, 4, 1098-1102.	0.7	23
314	Ultrafast Excitonic Behavior in Two-Dimensional Metal–Semiconductor Heterostructure. ACS Photonics, 2019, 6, 1379-1386.	3.2	23
315	Liquid Exfoliation of Icosahedral Quasicrystals. Advanced Functional Materials, 2018, 28, 1801181.	7.8	21
316	Effect of lattice stacking orientation and local thickness variation on the mechanical behavior of few layer graphene oxide. Carbon, 2018, 136, 168-175.	5.4	21
317	Tuning the Electrocatalytic Activity of Co ₃ O ₄ through Discrete Elemental Doping. ACS Applied Materials & Interfaces, 2019, 11, 39706-39714.	4.0	21
318	Twoâ€Dimensional Amorphous Cr 2 O 3 Modified Metallic Electrodes for Hydrogen Evolution Reaction. Physica Status Solidi - Rapid Research Letters, 2019, 13, 1900025.	1.2	21
319	Direct Cation Exchange in Monolayer <mml:math <br="" xmlns:mml="http://www.w3.org/1998/Math/MathML">display="inline"><mml:mrow><mml:msub><mml:mrow><mml:mi>MoS</mml:mi></mml:mrow><mml:mn>2via Recombination-Enhanced Migration. Physical Review Letters, 2019, 122, 106101.</mml:mn></mml:msub></mml:mrow></mml:math>	ml 2:0 9> <td>nn2l1msub><!--</td--></td>	nn 2l1 msub> </td
320	Corrosion Resistance of Sulfur–Selenium Alloy Coatings. Advanced Materials, 2021, 33, e2104467.	11.1	21
321	Friction of magnetene, a non–van der Waals 2D material. Science Advances, 2021, 7, eabk2041.	4.7	21
322	High Toughness in Ultralow Density Graphene Oxide Foam. Advanced Materials Interfaces, 2017, 4, 1700030.	1.9	20
323	Gate-Induced Metal–Insulator Transition in 2D van der Waals Layers of Copper Indium Selenide Based Field-Effect Transistors. ACS Nano, 2019, 13, 13413-13420.	7.3	20
324	Materials science perspective of multifunctional materials derived from collagen. International Materials Reviews, 2021, 66, 160-187.	9.4	20

#	Article	IF	CITATIONS
325	Atomic Layers of Graphene for Microbial Corrosion Prevention. ACS Nano, 2021, 15, 447-454.	7.3	20
326	Graphene Oxide Epoxy (GOâ€xy): GO as Epoxy Adhesive by Interfacial Reaction of Functionalities. Advanced Materials Interfaces, 2018, 5, 1700657.	1.9	19
327	Near-Field Coupled Integrable Two-Dimensional InSe Photosensor on Optical Fiber. ACS Nano, 2018, 12, 12571-12577.	7.3	19
328	Molecular Simulation of MoS2 Exfoliation. Scientific Reports, 2018, 8, 16761.	1.6	19
329	Recent Advances in Synthesis and Applications of 2D Junctions. Small, 2018, 14, e1801606.	5.2	19
330	Extraction of Two-Dimensional Aluminum Alloys from Decagonal Quasicrystals. ACS Nano, 2020, 14, 7435-7443.	7.3	19
331	An n-type, new emerging luminescent polybenzodioxane polymer for application in solution-processed green emitting OLEDs. Journal of Materials Chemistry C, 2015, 3, 2568-2574.	2.7	18
332	Indentation Tests Reveal Geometry-Regulated Stiffening of Nanotube Junctions. Nano Letters, 2016, 16, 232-236.	4.5	18
333	Dynamic mechanical analysis in materials science: The Novice's Tale. Oxford Open Materials Science, 2020, 1, .	0.5	18
334	Two-dimensional cobalt telluride as a piezo-tribogenerator. Nanoscale, 2022, 14, 7788-7797.	2.8	18
335	3D Printed Materials in Water Treatment Applications. Advanced Sustainable Systems, 2022, 6, .	2.7	18
336	Engineering Photophenomena in Large, 3D Structures Composed of Selfâ€Assembled van der Waals Heterostructure Flakes. Advanced Optical Materials, 2015, 3, 1551-1556.	3.6	17
337	Solid–Vapor Reaction Growth of Transitionâ€Metal Dichalcogenide Monolayers. Angewandte Chemie, 2016, 128, 10814-10819.	1.6	17
338	Direct Ink Writing of Cement Structures Modified with Nanoscale Additive. Advanced Engineering Materials, 2019, 21, 1801380.	1.6	17
339	Mechanistic insight into the improved Li ion conductivity of solid polymer electrolytes. RSC Advances, 2019, 9, 38646-38657.	1.7	17
340	Remote Lightening and Ultrafast Transition: Intrinsic Modulation of Exciton Spatiotemporal Dynamics in Monolayer MoS ₂ . ACS Nano, 2020, 14, 6897-6905.	7.3	17
341	Intrinsic coherence time of trions in monolayer <mml:math xmlns:mml="http://www.w3.org/1998/Math/MathML"><mml:msub><mml:mi>MoSe</mml:mi><mml:mn>2measured via two-dimensional coherent spectroscopy. Physical Review Materials, 2018, 2, .</mml:mn></mml:msub></mml:math 	ım l:non9 <td>nmlมวาsub><</td>	nml มว าsub><
342	<i>In vitro</i> cytotoxicity of functionalized single walled carbon nanotubes for targeted gene delivery applications. Nanotoxicology, 2008, 2, 184-188.	1.6	16

#	Article	IF	CITATIONS
343	Insight into In Situ Amphiphilic Functionalization of Few‣ayered Transition Metal Dichalcogenide Nanosheets. Advanced Materials, 2016, 28, 8469-8476.	11.1	16
344	Designing artificial 2D crystals with site and size controlled quantum dots. Scientific Reports, 2017, 7, 9965.	1.6	16
345	Multi-organ on a chip for personalized precision medicine. MRS Communications, 2018, 8, 652-667.	0.8	16
346	CoO Quantum Dots Anchored on Reduced Graphene Oxide Aerogels for Lithium-Ion Storage. ACS Applied Nano Materials, 2020, 3, 10369-10379.	2.4	16
347	Mapping Modified Electronic Levels in the Moiré Patterns in MoS ₂ /WSe ₂ Using Low-Loss EELS. Nano Letters, 2021, 21, 4071-4077.	4.5	16
348	Graphene Confers Ultralow Friction on Nanogear Cogs. Small, 2021, 17, 2104487.	5.2	16
349	Printing Highly Controlled Suspended Carbon Nanotube Network on Micro-patterned Superhydrophobic Flexible Surface. Scientific Reports, 2015, 5, 15908.	1.6	15
350	Photoresponse: Highly Sensitive Detection of Polarized Light Using Anisotropic 2D ReS ₂ (Adv. Funct. Mater. 8/2016). Advanced Functional Materials, 2016, 26, 1146-1146.	7.8	15
351	Scaleâ€Enhanced Magnetism in Exfoliated Atomically Thin Magnetite Sheets. Small, 2020, 16, e2004208.	5.2	15
352	Role of Atomic Layer Functionalization in Building Scalable Bottom-Up Assembly of Ultra-Low Density Multifunctional Three-Dimensional Nanostructures. ACS Nano, 2017, 11, 806-813.	7.3	14
353	Nature-Derived Sodium-Ion Battery: Mechanistic Insights into Na-Ion Coordination within Sustainable Molecular Cathode Materials. ACS Applied Energy Materials, 2019, 2, 8596-8604.	2.5	14
354	Atomic-Level Alloying of Sulfur and Selenium for Advanced Lithium Batteries. ACS Applied Materials & Interfaces, 2020, 12, 1005-1013.	4.0	14
355	Directly Exfoliated Ultrathin Silicon Nanosheets for Enhanced Photocatalytic Hydrogen Production. Journal of Physical Chemistry Letters, 2020, 11, 8668-8674.	2.1	14
356	Exploring the Possibility of βâ€Phase Arsenicâ€Phosphorus Polymorph Monolayer as Anode Materials for Sodiumâ€ion Batteries. Advanced Theory and Simulations, 2020, 3, 2000023.	1.3	14
357	2D Materials: Emerging Applications of Elemental 2D Materials (Adv. Mater. 7/2020). Advanced Materials, 2020, 32, 2070052.	11.1	14
358	Carrier-specific dynamics in 2H-MoTe2 observed by femtosecond soft x-ray absorption spectroscopy using an x-ray free-electron laser. Structural Dynamics, 2021, 8, 014501.	0.9	14
359	Carbon Nanotubesâ€Based Electrocatalysts: Structural Regulation, Support Effect, and Synchrotronâ€Based Characterization. Advanced Functional Materials, 2022, 32, 2106684.	7.8	14
360	TerraByte flash memory with carbon nanotubes. Applied Physics Letters, 2005, 86, 093106.	1.5	13

#	Article	IF	CITATIONS
361	Thermoplastic Polyurethane Nanocomposites Produced via Impregnation of Long Carbon Nanotube Forests. Macromolecular Materials and Engineering, 2011, 296, 53-58.	1.7	13
362	Origamiâ€Inspired 3D Interconnected Molybdenum Carbide Nanoflakes. Advanced Materials Interfaces, 2018, 5, 1701113.	1.9	13
363	A Study of Vertical Transport through Graphene toward Control of Quantum Tunneling. Nano Letters, 2018, 18, 682-688.	4.5	13
364	Strainâ€Induced Structural Deformation Study of 2D Mo <i>_x</i> W _{(1â€} <i>_x</i> ₎) S ₂ . Advanced Materials Interfaces, 2019, 6, 1801262.	1.9	13
365	High-K dielectric sulfur-selenium alloys. Science Advances, 2019, 5, eaau9785.	4.7	13
366	Fluorinated Boron Nitride Quantum Dots: A New 0D Material for Energy Conversion and Detection of Cellular Metabolism. Particle and Particle Systems Characterization, 2019, 36, 1800346.	1.2	13
367	Highly efficient photoelectric effect in halide perovskites for regenerative electron sources. Nature Communications, 2021, 12, 673.	5.8	13
368	Interferometric 4Dâ€STEM for Lattice Distortion and Interlayer Spacing Measurements of Bilayer and Trilayer 2D Materials. Small, 2021, 17, e2100388.	5.2	13
369	An Atomistic Tomographic Study of Oxygen and Hydrogen Atoms and their Molecules in CVD Grown Graphene. Small, 2015, 11, 5968-5974.	5.2	12
370	Reflux pretreatment-mediated sonication: A new universal route to obtain 2D quantum dots. Materials Today, 2019, 22, 17-24.	8.3	12
371	<i>Boxception</i> : Impact Resistance Structure Using 3D Printing. Advanced Engineering Materials, 2019, 21, 1900167.	1.6	12
372	Emerging Phases of Layered Metal Chalcogenides. Small, 2022, 18, e2105215.	5.2	12
373	Etching of transition metal dichalcogenide monolayers into nanoribbon arrays. Nanoscale Horizons, 2019, 4, 689-696.	4.1	11
374	Engineered 2D nanomaterials–protein interfaces for efficient sensors. Journal of Materials Research, 2015, 30, 3565-3574.	1.2	10
375	Effect of Oxygen Adsorbates on Terahertz Emission Properties of Various Semiconductor Surfaces Covered with Graphene. Journal of Infrared, Millimeter, and Terahertz Waves, 2016, 37, 1117-1123.	1.2	10
376	Simultaneous Preparation and Functionalization of 2D Materials Assisted by Amphiphilic MoS ₂ Nanosheets. Advanced Materials Interfaces, 2017, 4, 1600847.	1.9	10
377	Impurity-Controlled Crystal Growth in Low-Dimensional Bismuth Telluride. Chemistry of Materials, 2018, 30, 6108-6115.	3.2	10
378	Strong Effect of B-Site Substitution on the Reactivity of Layered Perovskite Oxides Probed via Isopropanol Conversion. , 2019, 1, 230-236.		10

#	Article	IF	CITATIONS
379	Electric Double Layer Field-Effect Transistors Using Two-Dimensional (2D) Layers of Copper Indium Selenide (CuIn7Se11). Electronics (Switzerland), 2019, 8, 645.	1.8	10
380	Three-Dimensional Extrusion Printing of Porous Scaffolds Using Storable Ceramic Inks. Tissue Engineering - Part C: Methods, 2020, 26, 292-305.	1.1	10
381	Gasâ€Phase Fluorination of Hexagonal Boron Nitride. Advanced Materials, 2021, 33, e2106084.	11.1	10
382	Metal-Free Sulfonate/Sulfate-Functionalized Carbon Nitride for Direct Conversion of Glucose to Levulinic Acid. ACS Sustainable Chemistry and Engineering, 2022, 10, 6230-6243.	3.2	10
383	Fluctuation enhanced gas sensing on functionalized carbon nanotube thin films. Physica Status Solidi (B): Basic Research, 2008, 245, 2339-2342.	0.7	9
384	Interconnecting Bone Nanoparticles by Ovalbumin Molecules to Build a Three-Dimensional Low-Density and Tough Material. ACS Applied Materials & Interfaces, 2018, 10, 41757-41762.	4.0	9
385	Selective Selenium-Substituted Metallic MoTe ₂ toward Ternary Atomic Layers with Tunable Semiconducting Character. Journal of Physical Chemistry C, 2019, 123, 24927-24933.	1.5	9
386	Deformation resilient cement structures using 3D-printed molds. IScience, 2021, 24, 102174.	1.9	9
387	Vertically aligned conductive carbon nanotube junctions and arrays for device applications. Applied Physics Letters, 2004, 84, 2889-2891.	1.5	8
388	Influences of organometallic polymer-derived catalyst dispersion on SWNT growth. Journal of Polymer Science, Part B: Polymer Physics, 2007, 45, 758-765.	2.4	8
389	Foamâ€Like Behavior in Compliant, Continuously Reinforced Nanocomposites. Advanced Functional Materials, 2013, 23, 3002-3007.	7.8	8
390	Correlation between types of defects/vacancies of Bi2S3 nanostructures and their transient photocurrent. Nano Research, 2017, 10, 2405-2414.	5.8	8
391	Structural Reinforcement through Liquid Encapsulation. Advanced Materials Interfaces, 2017, 4, 1600781.	1.9	8
392	Self‣tiffening Behavior of Reinforced Carbon Nanotubes Spheres. Advanced Engineering Materials, 2017, 19, 1600756.	1.6	8
393	Characterization of tin(II) sulfide defects/vacancies and correlation with their photocurrent. Nano Research, 2017, 10, 218-228.	5.8	8
394	Thermal Boundary Conductance and Phonon Transmission in Hexagonal Boron Nitride/Graphene Heterostructures. Physica Status Solidi (A) Applications and Materials Science, 2019, 216, 1900446.	0.8	8
395	Spontaneous Emission of Plasmonâ€Exciton Polaritons Revealed by Ultrafast Nonradiative Decays. Laser and Photonics Reviews, 2020, 14, 2000233.	4.4	8
396	Growth of highly crystalline ultrathin two-dimensional selenene. 2D Materials, 2022, 9, 045004.	2.0	8

#	Article	IF	CITATIONS
397	Enhancing Mechanical Properties of Nanocomposites Using Interconnected Carbon Nanotubes (<i>i</i> CNT) as Reinforcement. Advanced Engineering Materials, 2017, 19, 1600499.	1.6	7
398	Multifunctional Hybrids Based on 2D Fluorinated Graphene Oxide and Superparamagnetic Iron Oxide Nanoparticles. Particle and Particle Systems Characterization, 2017, 34, 1700245.	1.2	7
399	Influence of channel thickness on charge transport behavior of multi-layer indium selenide (InSe) field-effect transistors. 2D Materials, 2020, 7, 025030.	2.0	7
400	Investigating phase transitions from local crystallographic analysis based on statistical learning of atomic environments in 2D MoS2-ReS2. Applied Physics Reviews, 2021, 8, 011409.	5.5	7
401	Patterning, Transfer, and Tensile Testing of Covalent Organic Framework Films with Nanoscale Thickness. Chemistry of Materials, 2021, 33, 6724-6730.	3.2	7
402	Nanosupercapacitors with fractal structures: searching designs to push the limit. Journal of Materials Chemistry A, 2021, 9, 17400-17414.	5.2	7
403	High-Strength, Microporous, Two-Dimensional Polymer Thin Films with Rigid Benzoxazole Linkage. ACS Applied Materials & Interfaces, 2022, 14, 1861-1873.	4.0	7
404	Oxygen Reduction Reaction with Manganese Oxide Nanospheres in Microbial Fuel Cells. ACS Omega, 2022, 7, 11777-11787.	1.6	7
405	Carbon nanotube based sensors and fluctuation enhanced sensing. Physica Status Solidi C: Current Topics in Solid State Physics, 2010, 7, 1217-1221.	0.8	6
406	Solid–Liquid Self-Adaptive Polymeric Composite. ACS Applied Materials & Interfaces, 2016, 8, 2142-2147.	4.0	6
407	Increased solubility and fiber spinning of graphenide dispersions aided by crown-ethers. Chemical Communications, 2017, 53, 1498-1501.	2.2	6
408	Immunogenicity of Externally Activated Nanoparticles for Cancer Therapy. Cancers, 2020, 12, 3559.	1.7	6
409	Nature-Inspired Purpurin Polymer for Li-Ion Batteries: Mechanistic Insights into Energy Storage via Solid-State NMR and Computational Studies. Journal of Physical Chemistry C, 2020, 124, 17939-17948.	1.5	6
410	Transition pathways towards net-zero emissions methanol production. Green Chemistry, 2021, 23, 9844-9854.	4.6	6
411	Fiber-reinforced monolithic supercapacitors with interdigitated interfaces. Journal of Materials Chemistry A, 2021, 9, 11033-11041.	5.2	6
412	On the Interaction of Metal Nanoparticles with Supports. Topics in Catalysis, 2015, 58, 1127-1135.	1.3	5
413	Lattice Plasmon Induced Large Enhancement of Excitonic Emission in Monolayer Metal Dichalcogenides. Plasmonics, 2017, 12, 1975-1981.	1.8	5
414	Achieving Selfâ€Stiffening and Laser Healing by Interconnecting Graphene Oxide Sheets with Amineâ€Functionalized Ovalbumin. Advanced Materials Interfaces, 2018, 5, 1800932.	1.9	5

#	Article	IF	CITATIONS
415	Mxene Synthesis: HClâ€Based Hydrothermal Etching Strategy toward Fluorideâ€Free MXenes (Adv. Mater.) Tj E	TQq1] 0.	784 <u>3</u> 14 rgBT
416	Sustainable Biocomposites for Structural Applications with Environmental Affinity. ACS Applied Materials & Interfaces, 2022, 14, 17837-17848.	4.0	5
417	High Throughput Data-Driven Design of Laser-Crystallized 2D MoS ₂ Chemical Sensors: A Demonstration for NO ₂ Detection. ACS Applied Nano Materials, 2022, 5, 7549-7561.	2.4	5
418	Mechanical reliability of monolayer MoS2 and WSe2. Matter, 2022, 5, 2975-2989.	5.0	5
419	Alternating current-to-direct current power conversion by single-wall carbon nanotube diodes. Applied Physics Letters, 2010, 96, 233109.	1.5	4
420	Enabling Ultrasensitive Photo-detection Through Control of Interface Properties in Molybdenum Disulfide Atomic Layers. Scientific Reports, 2016, 6, 39465.	1.6	4
421	Room temperature 2D memristive transistor with optical short-term plasticity. , 2017, , .		4
422	Rational Design of Niâ€Based Electrocatalysts by Modulation of Iron Ions and Carbon Nanotubes for Enhanced Oxygen Evolution Reaction. Advanced Sustainable Systems, 2020, 4, 2000227.	2.7	4
423	Oxygenation of Diamond Surfaces via Hummer's Method. Chemistry of Materials, 2021, 33, 4977-4987.	3.2	4
424	Magnetite-Functionalized Plumbagin for Therapeutic Applications. ACS Sustainable Chemistry and Engineering, 2021, 9, 1361-1372.	3.2	4
425	Determining Quasiparticle Bandgap of Two-Dimensional Transition Metal Dichalcogenides by Observation of Hot Carrier Relaxation Dynamics. Journal of Physical Chemistry Letters, 2021, 12, 585-591.	2.1	4
426	Edgeâ€Mediated Annihilation of Vacancy Clusters in Monolayer Molybdenum Diselenide (MoSe ₂) under Electron Beam Irradiation. Small, 2022, 18, e2105194.	5.2	4
427	Quantum Materials Manufacturing. Advanced Materials, 2023, 35, e2109892.	11.1	4
428	Generation of intense phase-stable femtosecond hard X-ray pulse pairs. Proceedings of the National Academy of Sciences of the United States of America, 2022, 119, e2119616119.	3.3	4
429	Nanoscale Mapping and Defectâ€Assisted Manipulation of Surface Plasmon Resonances in 2D Bi ₂ Te ₃ /Sb ₂ Te ₃ Inâ€Plane Heterostructures. Advanced Optical Materials, 2022, 10, .	3.6	4
430	Energy Harvesting from Atomically Thin Co ₂ Te ₃ . Journal of Physical Chemistry C, 2022, 126, 12545-12553.	1.5	4
431	Temperature dependent high-bias electrical properties of C60 microrods. Journal of Applied Physics, 2008, 103, 064903.	1.1	3
432	Local charge transfer doping in suspended graphene nanojunctions. Applied Physics Letters, 2012, 100, 023306.	1.5	3

#	Article	IF	CITATIONS
433	Effect of microwave irradiation on carbon nanotube fibers: exfoliation, structural change and strong light emission. RSC Advances, 2014, 4, 15502-15506.	1.7	3
434	Electrocatalysts: Mass and Charge Transfer Coenhanced Oxygen Evolution Behaviors in CoFe-Layered Double Hydroxide Assembled on Graphene (Adv. Mater. Interfaces 7/2016). Advanced Materials Interfaces, 2016, 3, .	1.9	3
435	Phase Transformations During Li-Insertion into V2O5 at Elevated Temperature. Jom, 2017, 69, 1509-1512.	0.9	3
436	In Situ Study of High-Temperature Mechanical Properties of Carbon Nanotube Scaffolds. Microscopy and Microanalysis, 2017, 23, 782-783.	0.2	3
437	Strain-controlled optical transmittance tuning of three-dimensional carbon nanotube architectures. Journal of Materials Chemistry C, 2019, 7, 1927-1933.	2.7	3
438	Structural determination of Enzyme-Graphene Nanocomposite Sensor Material. Scientific Reports, 2019, 9, 15519.	1.6	3
439	Bioâ€Nanocomposite Coatings: Multifunctional Bioâ€Nanocomposite Coatings for Perishable Fruits (Adv.) Tj ETC	Qq] 10.78	843314 rgBT /(
440	Substitution of copper atoms into defect-rich molybdenum sulfides and their electrocatalytic activity. Nanoscale Advances, 2021, 3, 1747-1757.	2.2	3
441	One-Dimensional Hollow Structures of 2 <i>O</i> -PdS ₂ Decorated Carbon for Water Electrolysis. ACS Applied Energy Materials, 2021, 4, 8715-8720.	2.5	3
442	Stacked On-Chip Supercapacitors for Extreme Environments. Journal of Materials Chemistry A, 0, , .	5.2	3
443	Reversible separation of single-walled carbon nanotubes in bundles. Applied Physics Letters, 2008, 93, 083120.	1.5	2
444	Creating supersolvophobic nanocomposite materials. RSC Advances, 2013, 3, 4216.	1.7	2
445	Graphene Protein Field Effect Biomedical Sensor for Glucose Measurements. Materials Research Society Symposia Proceedings, 2015, 1725, 50.	0.1	2
446	Energy Storage: Superior Potassium Ion Storage via Vertical MoS ₂ "Nanoâ€Rose―with Expanded Interlayers on Graphene (Small 42/2017). Small, 2017, 13, .	5.2	2
447	Quaternary Alloys: Thermally Induced 2D Alloyâ€Heterostructure Transformation in Quaternary Alloys (Adv. Mater. 45/2018). Advanced Materials, 2018, 30, 1870344.	11.1	2
448	Intracellular microRNA quantification in intact cells: a novel strategy based on reduced graphene oxide-based fluorescence quenching. MRS Communications, 2018, 8, 642-651.	0.8	2
449	One Step Process for Infiltration of Magnetic Nanoparticles into CNT Arrays for Enhanced Field Emission. Advanced Materials Interfaces, 2018, 5, 1701631.	1.9	2
450	Good riddance, dendrites. Nature Energy, 2019, 4, 631-632.	19.8	2

#	Article	IF	CITATIONS
451	Interfacial States and Fano–Feshbach Resonance in Graphene–Silicon Vertical Junction. Nano Letters, 2019, 19, 6765-6771.	4.5	2
452	3D Printing: 3D Printed Tubulanes as Lightweight Hypervelocity Impact Resistant Structures (Small) Tj ETQq0 0	0 rgBT /Ove	erl <u>o</u> ck 10 Tf 5
453	A reactive molecular dynamics study of the hydrogenation of diamond surfaces. Computational Materials Science, 2021, 200, 110859.	1.4	2
454	AFM-Based Surface Potential Measurements on Carbon Nanotubes. Materials Research Society Symposia Proceedings, 2001, 706, 1.	0.1	1
455	Synthetic Approaches for Carbon Nanotubes. , 2005, , 33-55.		1
456	Effect of Sidewall Fluorination on the Mechanical Properties of Catalytically Grown Multi-Wall Carbon Nanotubes. Materials Research Society Symposia Proceedings, 2011, 1284, 157.	0.1	1
457	Hydrogels: Reversible Formation of g ₃ N ₄ 3D Hydrogels through Ionic Liquid Activation: Gelation Behavior and Roomâ€Temperature Gasâ€5ensing Properties (Adv. Funct. Mater.) Tj ETQq1 I	l 0. 7.8 4314	rgBT /Overlo
458	2D Materials: Quaternary 2D Transition Metal Dichalcogenides (TMDs) with Tunable Bandgap (Adv.) Tj ETQq0 0	0 rg₿Ţ /Ov	erlock 10 Tf S
459	2D Materials: Re Doping in 2D Transition Metal Dichalcogenides as a New Route to Tailor Structural Phases and Induced Magnetism (Adv. Mater. 43/2017). Advanced Materials, 2017, 29, .	11.1	1
460	Directly Identifying Phase Segregation in 2D Quaternary Alloys. Microscopy and Microanalysis, 2017, 23, 1438-1439.	0.2	1
461	Low Loss EELS of Lateral MoS ₂ /WS ₂ Heterostructures. Microscopy and Microanalysis, 2019, 25, 640-641.	0.2	1
462	Determining the 3D Atomic Coordinates and Crystal Defects in 2D Materials with Picometer Precision. Microscopy and Microanalysis, 2019, 25, 404-405.	0.2	1
463	Structural, Optical and Thermal Behavior investigation of 2D Bi2Te3/Sb2Te3 in-plane Heterostructures via Aberration Corrected STEM and EELS. Microscopy and Microanalysis, 2019, 25, 2012-2013.	0.2	1
464	Thermodynamics of order and randomness in dopant distributions inferred from atomically resolved imaging. Npj Computational Materials, 2021, 7, .	3.5	1
465	Stability of oxygenated groups on pristine and defective diamond surfaces. MRS Advances, 2022, 7, 543-546.	0.5	1
466	Attenuation of Surface Acoustic Waves by Carbon Nanotubes. Materials Research Society Symposia Proceedings, 2002, 750, 1.	0.1	0
467	Investigation on Site Density of Carbon Nanotube Forests. Materials Research Society Symposia Proceedings, 2007, 1018, 1.	0.1	0
468	Quantification of Dopant Distribution and the Local Band Gap in Selenium-Doped Molybdenum Disulfide. Microscopy and Microanalysis, 2014, 20, 1754-1755.	0.2	0

#	Article	IF	CITATIONS
469	Laser Terahertz Emission Spectroscopy of Graphene/InAs Junctions. Materials Research Society Symposia Proceedings, 2015, 1808, 1-7.	0.1	0
470	Interfaces in Two-Dimensional Heterostructures of Transition Metal Dichalcogenides. Microscopy and Microanalysis, 2015, 21, 105-106.	0.2	0
471	Photoemission Electron Microscopy as a New Tool to Study the Electronic Properties of 2D Crystals and Inhomogeneous Semiconductors. Microscopy and Microanalysis, 2017, 23, 1504-1505.	0.2	0
472	Electron Microscopy of Sulfur Selenium Alloy with High –K Dielectric Properties Microscopy and Microanalysis, 2019, 25, 492-493.	0.2	0
473	Bioderived Molecular Electrodes for Nextâ€Generation Energyâ€Storage Materials. ChemSusChem, 2020, 13, 2106-2106.	3.6	0
474	Photo Rechargeable Liâ€lon Batteries Using Nanorod Heterostructure Electrodes (Small 51/2021). Small, 2021, 17, .	5.2	0